2-Amino-6-furan-2-yl-4-substituted Nicotinonitriles as A_{2A} Adenosine Receptor Antagonists

Monica Mantri, Olivier de Graaf, Jacobus van Veldhoven, Anikó Göblyös, Jacobien K. von Frijtag Drabbe Künzel, Thea Mulder-Krieger, Regina Link, Henk de Vries, Margot W. Beukers, Johannes Brussee, and Adriaan P. IJzerman*

Leiden/Amsterdam Center for Drug Research, Division of Medicinal Chemistry, P.O. Box 9502, 2300 RA Leiden, The Netherlands

Received December 19, 2007

A_{2A} adenosine receptor antagonists usually have bi- or tricyclic N aromatic systems with varying substitution patterns to achieve desired receptor affinity and selectivity. Using a pharmacophore model designed by overlap of nonxanthine type of previously known A_{2A} antagonists, we synthesized a new class of compounds having a 2-amino nicotinonitrile core moiety. From our data, we conclude that the presence of at least one furan group rather than phenyl is beneficial for high affinity on the A_{2A} adenosine receptor. Compounds **39** (LUF6050) and **44** (LUF6080) of the series had K_i values of 1.4 and 1.0 nM, respectively, with reasonable selectivity toward the other adenosine receptor subtypes, A_1, A_{2B}, and A_3. The high affinity of **44** was corroborated in a cAMP second messenger assay, yielding subnanomolar potency for this compound.

Introduction

Adenosine receptors have adenosine as their endogenous ligand and they belong to the class of G protein-coupled receptors (GPCRs). They occur as four different subtypes, A_1, A_{2A}, A_{2B}, and A_3, all of which have been cloned successfully into artificial cell lines. All adenosine receptors are associated with the cAMP[a] second messenger system. Activation of A_1 and A_3 receptors mediates inhibition of adenylate cyclase, while A_{2A} and A_{2B} receptors, when activated, increase the intracellular cyclic AMP level. In contrast to the widespread distribution of A_1 and A_{2B} receptors in the brain, the A_{2A} receptor is highly expressed only in striatum, nucleus accumbens, olfactory tubercles, and globus pallidus pars externa in the rat and human brain.[1] The A_{2A} receptor is coexpressed with D_2 receptors in striatum. It is involved in the regulation of functional activity of D_2 dopamine receptors[2] as heterodimerization of A_{2A} and D_2 receptor subtypes inhibits D_2 receptor functions. It has been found that A_{2A} adenosine receptor antagonists improve motor function in animal models of basal ganglia disorders. Thus, such compounds are thought to serve as a therapeutic modality in Parkinson's disease.

Previously known A_{2A} antagonists can be generally classified as xanthine-like and nonxanthine like structures. KW-6002 (istradefylline) is a xanthine derivative having a styryl moiety on the 8 position and is already in phase III clinical trials for the treatment of Parkinson's disease[3] (Figure 1). The 8-styryl xanthine moiety is associated with photochemical instability;[4] however, also, xanthine-based structures have already been optimized and explored to a high extent. This led us to find new plausible A_{2A} antagonists from nonxanthine like structures. In this paper, we report the synthesis and SAR of a new class of A_{2A} antagonists from a pharmacophore model, which we constructed using previously reported A_{2A} nonxanthine antagonists.

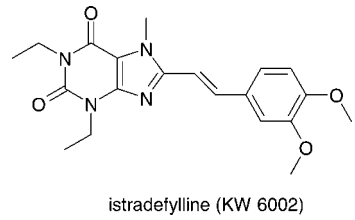

Figure 1. Istradefylline (KW-6002).

Results and Discussion

Molecular Modeling. A molecular superimposition model was constructed using previously published antagonist ligands having high affinity and selectivity for the A_{2A} adenosine receptor. All these molecules were selected with the criteria of having diverse scaffolds based on the heterocyclic aromatic core of each molecule. The actual ligand taken from a specific scaffold class was the one that had a combination of high affinity and selectivity for the A_{2A} adenosine receptor. We also included in the overlap four prototypic nonxanthine A_{2A} adenosine receptor antagonists, viz. CGS15943 (in fact a nonselective compound), 8FB-PTP, SCH58261, and ZM241385.

The molecules shown in Figure 2 were drawn in the SPARTAN '04[21] molecular modeling package, and each molecule was energy-minimized to yield the lowest energy conformer. Their electrostatic potentials were sampled over the entire Van der Waal's surface of each molecule and then electron density was mapped over it. As an example, SCH58261 is shown in Figure 3: shades of red and blue indicate relative electronegative and electropositive regions, respectively. After plotting the electrostatic potential over each individual molecule, we noticed that all of them share common features, i.e., an electron deficient region (blue) on the "top" of the molecule, accompanied by an electron rich region (red) on the "right-hand" side of the molecule. The former represents the H-bond donating free amino group in most of the cases, while the latter usually constitutes the electron rich region of the oxygen atom in a furan ring.

All molecules were superimposed on each other by considering these two areas of electron density together with the aromatic

* To whom correspondence should be addressed. Phone: +31 (0)71 527 4651. Fax: +31 (0)71 527 4565. E-mail: ijzerman@lacdr.leidenuniv.nl.

[a] Abbreviations: GPCR, G-protein-coupled receptor; cAMP, cyclic adenosine monophosphate; SAR, structure−activity relationship; CHO, chinese hamster ovary; HEK, human embryonic kidney; ADA, adenosine deaminase; AB-MECA, N^6-(4-aminobenzyl)adenosine-5′-methyluronamide; CPA, N^6-cyclopentyladenosine; DPCPX, 1,3-dipropyl-8-cyclopentylxanthine; NECA, 5′-*N*-ethylcarboxamidoadenosine; TLC, thin layer chromatography.

10.1021/jm701594y CCC: $40.75
Published on Web 07/19/2008

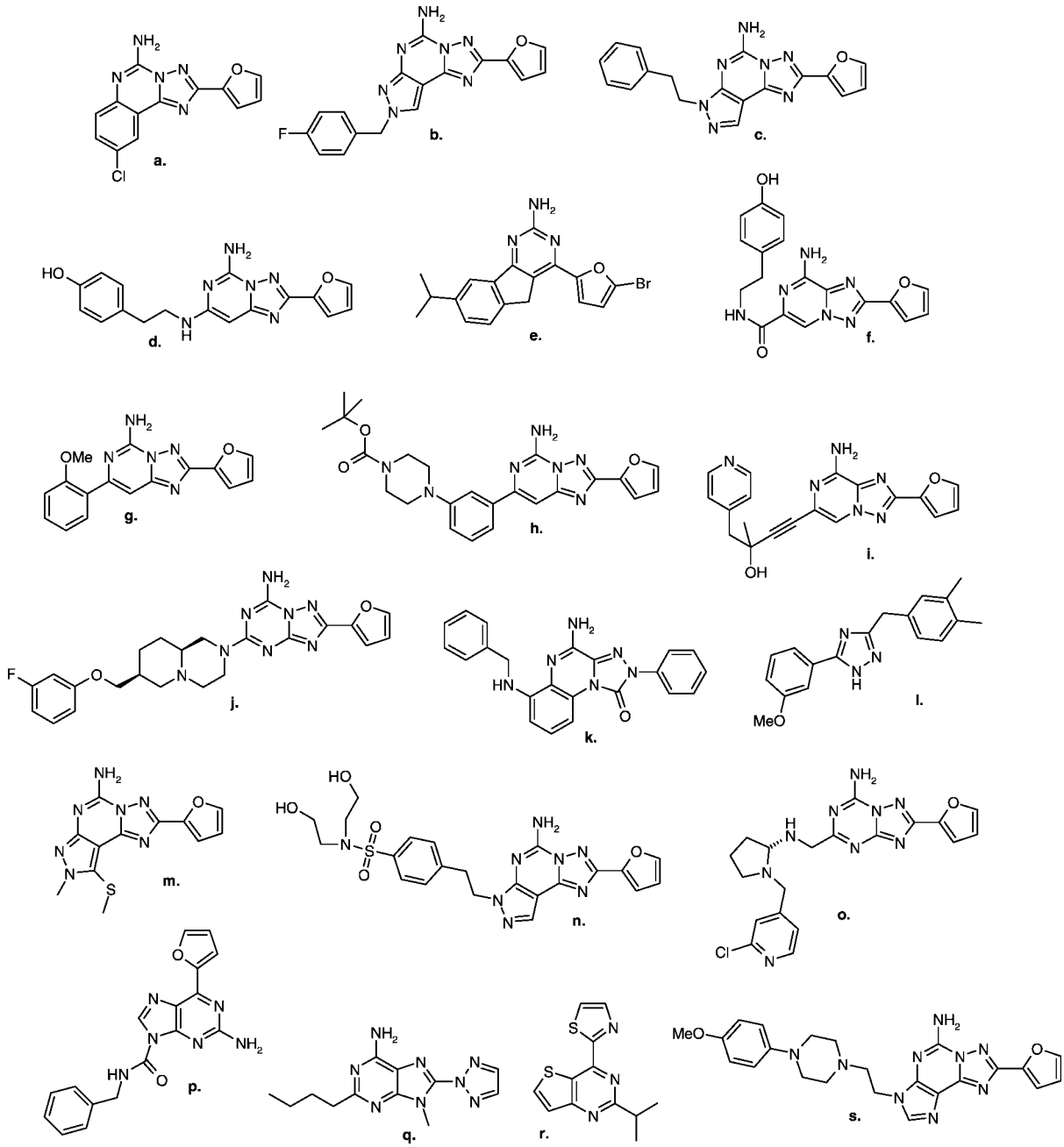

Figure 2. Set of molecules selected for their different scaffold structure. **a** CGS15943 K_i (hA_{2A}) = 0.4 nM,[5] **b** 8FB-PTP, **c** SCH58261 K_i (hA_{2A}) = 0.6 nM,[5] **d** ZM241385 K_i (hA_{2A}) = 0.8 nM,[5] **e** K_i (hA_{2A}) = 0.8 nM,[6] **f** K_i (rA_{2A}) = 1 nM,[7] **g** K_i (hA_{2A}) = 4.3 nM,[8] **h** K_i (hA_{2A}) = 0.5 nM,[9] **i** K_i (hA_{2A}) = 1.1 nM,[10] **j** K_i (hA_{2A}) = 0.2 nM,[11] **k** K_i (hA_{2A}) = 6.5 nM,[12] **l** K_i (hA_{2A}) = 20 nM,[13] **m** K_i (hA_{2A}) = 1.2 nM,[14] **n** K_i (hA_{2A}) = 0.12 nM,[15] **o** K_i (hA_{2A}) = 4 nM,[16] **p** K_i (hA_{2A}) = 1.1 nM,[17] **q** K_i (hA_{2A}) = 6.6 nM,[18] **r** K_i (hA_{2A}) = 1.4 nM,[19] **s** K_i (hA_{2A}) = 0.1 nM.[20]

nitrogen-containing ring system as a further basis of overlap (Figure 4a). Because molecules **c**, **d**, **f**, **h**, **i**, **k**, **n**, **s**, and **o** (Figure 2) had bulky and flexible side chains, the orientation of these side chains, at the "left side" of the molecules, was very diverse (Figure 4a). To enhance the model for better overlap in this region, the single conformation of each of the molecules mentioned above compatible with the best overlap was chosen from the set of all possible conformers within a limit of 5 kcal/mol above the lowest energy conformation (see Experimental Section for details). These selected conformations were overlapped with the other molecules used in the superimposition from Figure 4a to yield Figure 4b. A simplified version with only four molecules (**e**, **j**, **m**, and **r**) is shown in Figure 5 in which the electrostatic potential energy surface of **m** was chosen to show the general pattern of superimposition.

Superimposition of these molecules led to a pharmacophore model shown in Figure 6. From the superimposition, it is clear that for a molecule to be an A_{2A} adenosine receptor antagonist, it requires a hydrogen bond donor (A) and electron rich regions (B and C), present on an *N*-containing aromatic ring (A and B) and a largely lipophilic L_1 group (C). These areas comply with the recently published 3D pharmacophore model for A_{2A} receptor antagonism by Wei et al.[22] In addition to these regions, the *N*-containing ring also possesses an H-bond accepting region D. Furthermore, the lipophilic region L_2 seems to be desirable for good binding to the receptor. To this area an appropriately oriented heteroatom may be added (see also Figure 4b).

We decided to explore a monocyclic core ring structure in particular because very few A_{2A} adenosine receptor antagonists with such a scaffold have been reported (compound **l** in Figure

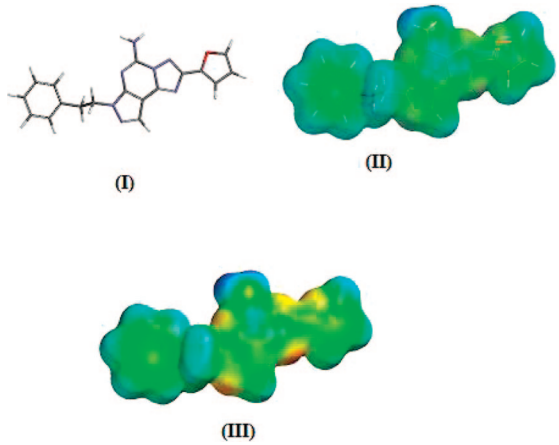

Figure 3. (I) SCH58261 in its lowest energy conformer as calculated with SPARTAN. (II) SCH58261 with electrostatic potential energy surface mapped as transparent cloud around stick model. (III) Molecular electrostatic potential energy surface of SCH58261.

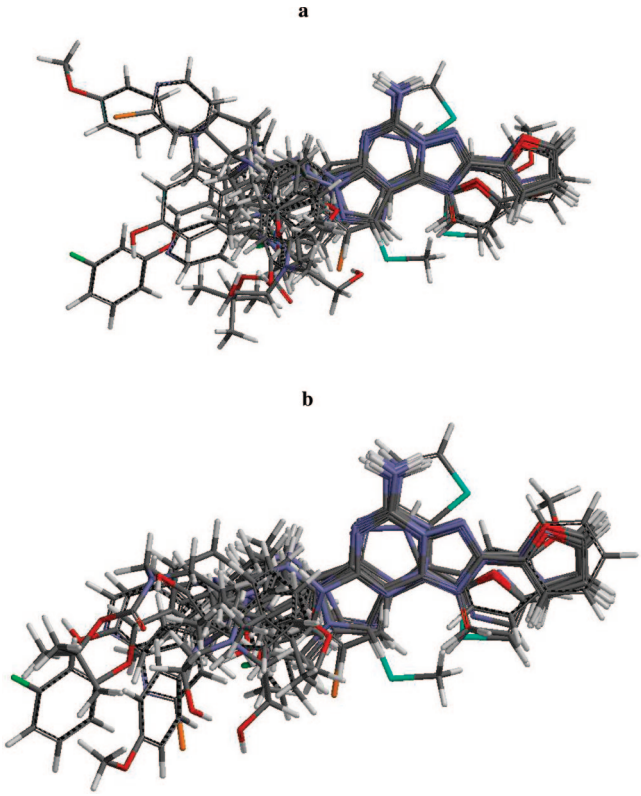

Figure 4. (a) Superimposition of all the molecules in their lowest energy conformation. (b) Optimized superimposition of molecules after selecting a conformer with better overlap in L_2 lipophilic region for highly flexible molecules.

2 is one of the few examples). From the pharmacophore model in Figure 6, we learned that a monocyclic ring should have an aromatic character and a nitrogen atom at position B. At position D, we chose the nitrile function instead of an extra nitrogen atom in the ring to obtain a better distance separation between D and C. For exploring lipophilic region L_1, we tried various aromatic rings with substitutions that are discussed later in Table 1 and Table 2 Thus we came up with the nicotinonitrile template, having an amino group at position 2 as an H-bond donor. For the exploration of lipophilic region L_1, we included various aromatic rings that are discussed later in Table 2. It has been recently reported by Richardson et al.[23] that a furan group may

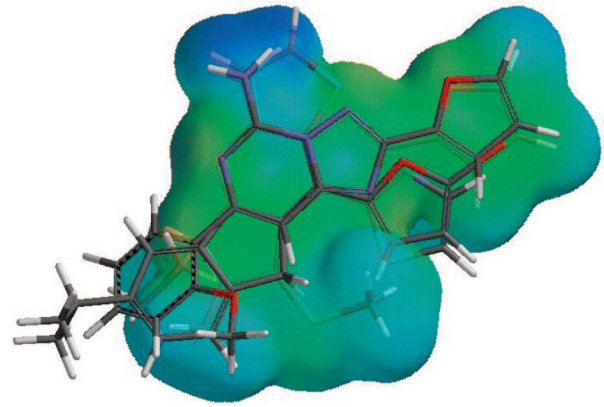

Figure 5. A simplified picture showing only four of the antagonists (**e**, **j**, **m**, **r**) superimposed on each other, also showing the electrostatic potential energy surface of **m**.

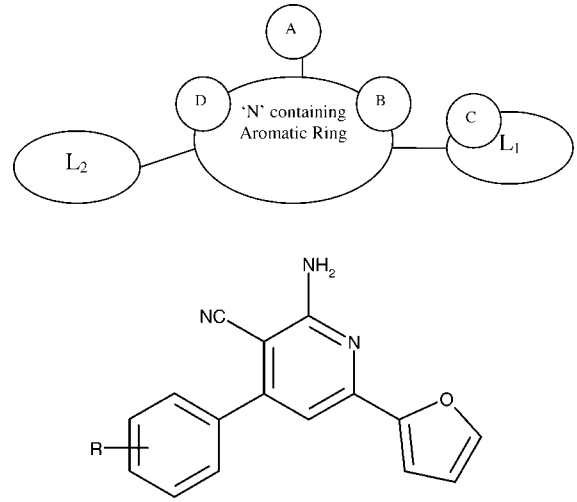

Figure 6. Simplified pharmacophore derived from superimposition of the investigated molecules. A represents a H-bond donating region, B, C and D represent electron-rich and H-bond accepting regions, respectively. L_1 and L_2 represent lipophilic regions. A molecule with a simple, monocyclic core and obeying the pharmacophore is shown below it.

carry a safety liability as it is prone to oxidative metabolism, hence we also searched for other rings at the L_1 lipophilic region.

Chemistry. The compounds were synthesized according to Scheme 1.[24] The aldehyde was reacted with malononitrile by adding a few drops of piperidine to give reaction intermediates **1**−**16** according to a Knoevenagel condensation.[25] In the case of heteroaromatic aldehydes, reactions were carried out at room temperature so as to avoid decomposition of the intermediate. In the next step, the malononitrile derivative and an aromatic acetyl ketone were fused with ammonium acetate in a microwave reactor at 120 °C for 1 h to form the nicotinonitriles **17**−**45**.[26] The reaction was optimized for microwave conditions for this temperature and time to give maximum yield. The final product was purified by column chromatography and recrystallization.

Structure−Activity Relationships. The results of radioligand binding assays performed on the substituted nicotinonitriles **17**−**45** are shown in Table 1.

The unsubstituted phenyl derivative (**17**) had 11 nM affinity for the A_{2A} receptor but was not much selective against the A_1 receptor (K_i = 28 nM). It also showed 170 nM affinity for the A_{2B} receptor. The biphenyl derivative **18** was inactive at both

Table 1. Affinities of 2-Amino-4,6-substituted Nicotinonitriles in Radioligand Binding Assays of Human Adenosine Receptors

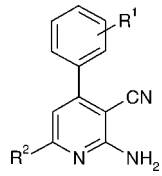

compound	R^1	R^2	K_i (nM) or % displacement[a]			
			hA_1[b]	hA_{2A}[c]	hA_{2B}[d]	hA_3[e]
17	H	furan-2-yl	28 ± 7	11 ± 5	170 ± 39	28%
18	4-phenyl	furan-2-yl	0%	0%	17%	4%
19	4-Cl	furan-2-yl	48 ± 7	140 ± 35	33%	21%
20	3,4-diCl	furan-2-yl	68 ± 23	190 ± 35	12%	14%
21	4-CH_3	furan-2-yl	47%	45%	15%	21%
22	4-OCH_3	furan-2-yl	34 ± 11	41 ± 6	33%	21%
23	3,4-diOCH_3	furan-2-yl	250 ± 99	92 ± 4	31%	20%
24	3,4-OCH_2O-	furan-2-yl	11 ± 2	26 ± 2	24%	390 ± 110
25	4-OH	furan-2-yl	54 ± 18	41 ± 15	370 ± 52	34%
26	4-$N(CH_3)_2$	furan-2-yl	11%	3.8%	2%	17%
27	4-$OCH(CH_3)_2$	furan-2-yl	19%	6%	8%	7%
28	3-OCF_3	furan-2-yl	270 ± 24	260 ± 13	29%	13%
29	3-CH_3	furan-2-yl	64 ± 18	140 ± 60	620 ± 220	18%
30	H	phenyl	14 ± 1	130 ± 10	26%	53%
31	3,4-diOCH_3	phenyl	66 ± 39	160 ± 10	13%	32%
32	3,4-OCH_2O-	phenyl	7.0 ± 0.4	34%	0%	48%
33	4-$N(CH_3)_2$	phenyl	12%	1%	4%	2%
34	3-OCF_3	phenyl	34 ± 2	58 ± 6	7%	28%
35	3-CH_3	phenyl	15 ± 1.5	130 ± 10	37%	33%
36	4-OH	phenyl	61 ± 19	17%	18%	18%
NECA			7.8 ± 0.7		1270 ± 160	11 ± 1
CPA			10 ± 1.3	1700 ± 300		280 ± 60
DPCPX			6.1 ± 1.6	130 (n = 2)		1700 ± 170

[a] K_i ± SEM (n = 3), % displacement (n = 2). [b] Displacement of specific [^{3}H]DPCPX binding in CHO cell membranes expressing human adenosine A_1 receptors or % displacement of specific binding at 1 μM concentrations. [c] Displacement of specific [^{3}H]ZM241385 binding in HEK293 cell membranes expressing human adenosine A_{2A} receptors or % displacement of specific binding at 1 μM concentrations. [d] Displacement of specific [^{3}H]MRS1754 binding in CHO cell membranes expressing human adenosine A_{2B} receptors or % displacement of specific binding at 1 μM concentrations. [e] Displacement of specific [^{125}I]AB-MECA binding in HEK293 cell membranes expressing human adenosine A_3 receptors or % displacement of specific binding at 1 μM concentrations.

Table 2. Affinities of 2-Amino-4,6-heteroaromatic-substituted Nicotinonitriles in Radioligand Binding Assays of Human Adenosine Receptors

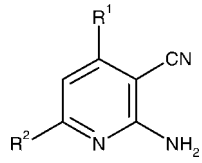

compound	R^1	R^2	K_i (nM) or % displacement[a]			
			hA_1[b]	hA_{2A}[c]	hA_{2B}[d]	hA_3[e]
37	furan-2-yl	phenyl	5.8 ± 1.5	19 ± 1	220 ± 40	29%
38	thiophen-2-yl	thiophen-2-yl	43 ± 6	32 ± 15	19%	31%
39	thiophen-2-yl	furan-2-yl	28 ± 6	1.4 ± 0.2	75 ± 15	51%
40	phenyl	thiophen-2-yl	12 ± 2	88 ± 25	41%	32%
41	phenyl	pyrrol-2-yl	28%	640 ± 370	35%	0%
42	furan-2-yl	thiophen-2-yl	29 ± 5	12 ± 1	380 ± 90	39%
43	thiophen-2-yl	phenyl	22 ± 10	54 ± 3	44%	11%
44	furan-2yl	furan-2-yl	12 ± 2	1.0 ± 0.1	34 ± 2	33%
45	5-Me-furan-2-yl	furan-2-yl	100 ± 30	15 ± 1	440 ± 110	24%

[a] K_i ± SEM (n = 3), % displacement (n = 2). [b] Displacement of specific [^{3}H]DPCPX binding in CHO cell membranes expressing human adenosine A_1 receptors or % displacement of specific binding at 1 μM concentrations. [c] Displacement of specific [^{3}H]ZM241385 binding in HEK293 cell membranes expressing human adenosine A_{2A} receptors or % displacement of specific binding at 1 μM concentrations. [d] Displacement of specific [^{3}H]MRS1754 binding in CHO cell membranes expressing human adenosine A_{2B} receptors or % displacement of specific binding at 1 μM concentrations. [e] Displacement of specific [^{125}I]AB-MECA binding in HEK293 cell membranes expressing human adenosine A_3 receptors or % displacement of specific binding at 1 μM concentrations.

A_{2A} and A_1 receptors, indicating that the L_2 pocket cannot accommodate extended bulky lipophilic groups. Further systematic evaluation of substitutions as suggested from the Topliss scheme[27] provided detailed insight in the requirements for A_{2A} adenosine receptor affinity. Both chloro substitution at the para position (**19**) and 3,4-dichloro substitution (**20**) reduced affinity for the A_{2A} and A_1 receptors as compared to unsubstituted **17**. Further changing substitution to methyl at the para position on the phenyl ring (**21**) appeared even more unfavorable with respect to affinity for A_{2A} and A_1 receptors with a displacement of radioligand of only 45% and 47%, respectively, at a concentration of 1 μM. Apparently, increased hydrophobicity and electron withdrawing character are detrimental for the affinity for the A_{2A} receptor. The introduction of a 4-methoxy

Scheme 1. Synthetic Route to 2-Amino-4,6-substituted Nicotinonitriles[a]

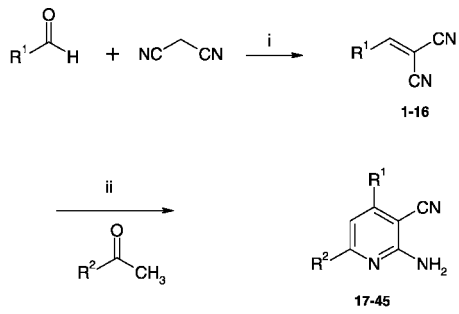

	R^1	R^2		R^1	R^2
17	Ph	2-Furyl	**31**	3,4-diOMe-Ph	Phenyl
18	4-Ph-Ph	2-Furyl	**32**	3,4-OCH_2O-Ph	Phenyl
19	4-Cl-Ph	2-Furyl	**33**	4-$N(Me)_2$-Ph	Phenyl
20	3,4-diCl-Ph	2-Furyl	**34**	3-OCF_3-Ph	Phenyl
21	4-Me-Ph	2-Furyl	**35**	3-Me-Ph	Phenyl
22	4-OMe-Ph	2-Furyl	**36**	4-OH-Ph	Phenyl
23	3,4-diOMe-Ph	2-Furyl	**37**	2-Furyl	Phenyl
24	3,4-OCH_2O-Ph	2-Furyl	**38**	Thiophen-2-yl	Thiophen-2-yl
25	4-OH-Ph	2-Furyl	**39**	Thiophen-2-yl	2-Furyl
26	4- $N(Me)_2$-Ph	2-Furyl	**40**	Phenyl	Thiophen-2-yl
27	4-OiPr-Ph	2-Furyl	**41**	Phenyl	2-Pyrrolyl
28	3-OCF_3-Ph	2-Furyl	**42**	2-Furyl	Thiophen-2-yl
29	3-Me-Ph	2-Furyl	**43**	Thiophen-2-yl	Phenyl
30	Ph	Phenyl	**44**	2-Furyl	2-Furyl
			45	5-Me-2-Furyl	2-Furyl

[a] Reagents and conditions: (i) Piperidine, EtOH, 1 h reflux; (ii) NH_4OAc, toluene, 120 °C in microwave.

group on the phenyl ring (**22**) showed restored affinity for the A_{2A} receptor but without selectivity against the A_1 receptor (K_i values of 41 nM and 34 nM, respectively). The 3,4-dimethoxy derivative **23** did show improvement in selectivity with respect to the A_1 receptor (K_i = 250 nM), however, its affinity for the A_{2A} receptor was decreased to 92 nM. On the other hand, compound **24** with a 3,4-dioxymethylene substituent showed 11 nM affinity for A_1 and 26 nM affinity for the A_{2A} receptor, indicating the subtle receptor interactions at this part of the molecule.

Compound **25** also displayed nanomolar affinity but less selectivity (41 nM for the A_{2A} and 54 nM for the A_1 receptor). Substitution at the para position by dimethyl amine (**26**) or an isopropoxy group (**27**) showed a complete loss of affinity for A_{2A} and A_1 receptors, again indicating that bulky groups in the L_2 pocket are not favorable. Compounds **28** and **29**, which have trifluoromethoxy and methyl groups at the meta position, respectively, showed 260 and 140 nM affinity for the A_{2A} adenosine receptor. However, these compounds were not selective as their affinity values for A_1 receptor were 270 nM (**28**) and 64 nM (**29**). Compounds **30**−**36** were synthesized to compare 2-amino-2-yl-6-furyl nicotinonitriles with 2-amino-2-yl-6-phenyl nicotinonitriles. Compound **30** with two phenyl substituents showed 14 nM affinity for the A_1 and 130 nM affinity for the A_{2A} receptor. These data compare unfavorably with furan-substituted **17**, suggesting that the presence of a furan moiety in the L_1 pocket is preferred for A_{2A} receptor affinity. This observation also holds true in case of the 3,4-dimethoxy substituent; the affinity of **23** changed from 92 to 160 nM after replacing the furan by a phenyl ring (**31**). In the case of the dioxymethylene ring, the change was even more prominent as compound **32** showed only 34% displacement of the A_{2A} receptor radioligand. Substitution at the para position by dimethyl amine (**33**) in the case of the phenyl series, also caused a complete loss of affinity for A_{2A} and A_1 receptors due to the unfavorable interaction with the bulky groups in the L_2 pocket. Compound **34** with a trifluoromethoxy substituent at the meta position on the phenyl ring showed an affinity of 34 nM for A_1 and 58 nM for A_{2A} adenosine receptors. This represented improved affinity over its furan analogue (**28**), but no significant difference in selectivity was observed. The *meta*-methyl-substituted derivative (**35**) actually showed more selectivity toward A_1 as compared to A_{2A} adenosine receptors with a K_i value 15 nM for A_1 and 130 nM for A_{2A} receptors. Compound **36** with a *para*-substituted hydroxy group on the phenyl ring showed almost complete loss of affinity (17% displacement only at 1 μM) for A_{2A} adenosine receptor. Comparing **36** with **25** is another confirmation that in case of nicotinonitriles the presence of a furan ring in the L_1 pocket is preferred over a phenyl ring with respect to A_{2A} adenosine receptor affinity. Concluding, the L_2 region can be substituted with various phenyl substituents. However, in most cases, the selectivity for the A_{2A} receptor is decreased in favor of the A_1 receptor.

Table 2 shows the results of radioligand binding assays performed on heteroaromatic substituted nicotinonitriles (**37**−**45**).

We optimized the L_1 and L_2 regions of the pharmacophore by substituting the core molecule with various combinations of heteroaromatic ring systems. All compounds had affinities for A_{2A} receptors in the low nanomolar range. Compounds **37** and **43**, however, displayed even higher affinity toward A_1 than A_{2A} receptors with K_i values of 5.8 and 19 nM for **37** and 22 and 54 nM for **43**. Compound **38** with two thiophene rings had 32 nM affinity for the A_{2A} adenosine receptor but was not selective (43 nM on the A_1 receptor). Replacing one of the rings by furan as in **39** and **42** rendered these molecules more selective against the A_1 receptor. The K_i values of **39** and **42** for the A_{2A} adenosine receptor were 1.4 and 12 nM with 20- and 2.4-fold selectivity, respectively. Also, compound **39** showed 75 nM affinity for the A_{2B} adenosine receptor. The only pyrrole derivative made in this series (**41**) displaced only 28% of the A_1 receptor radioligand, making it selective for A_{2A}, but its K_i value for this receptor subtype was modest (640 nM). These findings suggest that a five-membered heterocyclic ring is favored over a phenyl ring in the L_1 region, preferably with an H-bond accepting rather than donating heteroatom. Compound **44** with two furan rings yielded the highest affinity in this series for the A_{2A} receptor with a K_i value of 1.0 nM and 12-fold selectivity against the A_1 receptor. It also displayed 34-fold selectivity against the A_{2B} receptor (34 nM affinity). Recently, compound **44** has also been described as an inhibitor of mitogen-activated protein kinase-activated protein kinase-2.[28] Compound **45** with a 5-methyl substituent on the furan ring in the L_2 pocket showed somewhat reduced affinity for the A_{2A} (15 nM) and A_1 adenosine receptor (100 nM). However, this substituted furan group is more metabolically stable and might thus be preferred over the simple furan moiety. Other less "reactive" heterocyclic moieties may also be explored, although the furan ring per se is a very common feature in A_{2A}-selective adenosine receptor antagonists as found in many different research programs.

All compounds listed in both tables displayed little affinity for the human A_3 receptor. In most cases, there was less than 50% displacement of radioligand when compounds were tested at 1 μM concentration.

Functional Assay at A_{2A} Adenosine Receptors. For a functional evaluation, intact CHO cells expressing the human adenosine A_{2A} receptor were used. The cells were stimulated with increasing concentrations of the prototypic A_{2A} receptor agonist CGS21680 (2-[4-(2-carboxyethyl)phenylethylamino]-5′-*N*-ethylcarboxamidoadenosine). Further CGS21680 concentration−effect curves were recorded (n = 3) in the presence of two concentrations (10 and 100 nM) of **44** (Figure 7), causing

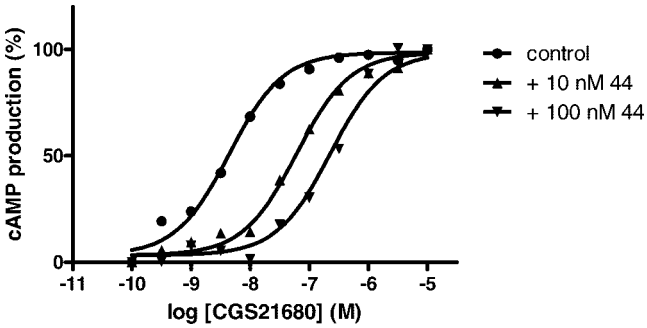

Figure 7. The effect of increasing concentrations of compound 44 (10 and 100 nM) on the cAMP production induced by increasing concentrations of CGS21680 in HEK 293 cells expressing the human A_{2A} adenosine receptor.

a rightward shift. These data were analyzed according to Gaddum and Schild, yielding a pA_2 value of 9.87 ± 0.36, corresponding to an apparent affinity (K_B value) of 0.14 nM for **44**. This value is in fair agreement with the binding data (K_i value of 1 nM).

Conclusion

In this paper, we presented a new series of 2-amino-6-furan-2-yl-4-substituted nicotinonitriles, designed and synthesized on the basis of a pharmacophore model derived through molecular modeling of previously known ligands. Comparing this series of compounds with a number of 2-amino-6-phenyl-2-yl-4-substituted nicotinonitriles demonstrated the importance of the furan moiety to render these nicotinonitriles potent for the A_{2A} adenosine receptor. Compound **44** is highly potent on this adenosine receptor subtype in both a radioligand binding and a second messenger assay. One possible advantage of these small molecules over some of the polycyclic antagonists resides in their more favorable physicochemical properties. With the Molecular Evoluator software,[29,30] the following parameters for compound **44** were calculated: LogP 3.06; MW 251; hydrogen bond acceptors 5; hydrogen bond donors 2. These values comply with the often-used Lipinski Rule of Five.[31]

Experimental Section

Molecular Modeling. Molecular modeling was performed with the SPARTAN '04[21] software package (Wave Function Inc.). Default values in the Merck Force field were used in molecular mechanics minimizations. Conjugate gradient energy minimization was continued until the rms energy derivative was less than 0.001 $kcal \cdot mol^{-1}$ $Å^{-1}$. Conformers were generated using the systematic search method, and the lowest energy conformer was used for further calculations. The molecular electrostatic potential of these conformers was calculated with the semiempirical molecular orbital program AM1. The energy and molecular electrostatic potentials were sampled over the entire accessible surface of the molecules (equal to the van der Waals contact surface). In the figures, the most negative electrostatic potential is colored red and the most positive one is blue.

For molecules **c**, **d**, **f**, **h**, **i**, **k**, **n**, **s**, and **o**, all possible conformations were generated by calculating their conformation distribution at ground-state by molecular mechanics. All the conformations for each molecule were sorted on the basis of the energy parameter to which a cutoff value of 5 kcal/mol from the lowest energy was applied. From the remaining conformers, one was chosen that had a side chain orientation that was most compatible with rigid compound **j** in Figure 2.

Chemistry, Materials, and Methods. All reagents were obtained from commercial sources and all solvents were of analytical grade. ^1H and ^{13}C NMR spectra were recorded on a Bruker AC 200 (^1H NMR, 200 MHz; ^{13}C NMR, 50.29 MHz) spectrometer with tetramethylsilane as an internal standard. Chemical shifts are reported in δ (ppm). Melting points were determined by Büchi melting point apparatus and are uncorrected. Elemental analyses were performed by Leiden Institute of Chemistry and are within 0.4% of theoretical values unless otherwise stated. Reactions were routinely monitored by TLC using Merck silica gel F_{254} plates. Microwave reactions were performed on an Emrys Optimizer (Biotage AB). Wattage was automatically adjusted to maintain the desired temperature.

General Procedure for the Preparation of Malononitriles (1−16). To malononitrile (20 mmol) dissolved in EtOH (40 mL) was added an aromatic aldehyde (20 mmol) followed by 2 drops of piperidine. In the case of substituted benzaldehydes, the reaction mixture was refluxed for 1 h. In the case of heterocyclic aromatic aldehydes, the reaction was carried out for 1 h at room temperature. The precipitate was formed on cooling the reaction mixture to room temperature. The crude product was filtered, and it was fairly pure to carry out the further reactions.

General Procedure for the Preparation of Nicotinonitriles (17−45). To a solution of previously synthesized benzylidene malononitrile (3 mmol, 1 equiv) in toluene was added 2-acetyl furan (3 mmol, 1 equiv) and ammonium acetate (4.5 mmol, 1.5 equiv). The mixture was heated in a microwave at 120 °C for 1 h. The reaction mixture was purified by column chromatography using dichloromethane−methanol solvent system. Recrystallization from methanol or ethanol gave the corresponding nicotinonitrile in pure form. The yield of reaction varied from 40−70%.

2-Amino-4-thiophen-2-yl-6-furan-2-yl-nicotinonitrile (39, LUF6050). mp: 180 °C. ^1H NMR $\delta(CDCl_3)$: 5.36 (s, 2H), 6.55−6.58 (m, 1H), 7.21 (s, 1H), 7.12−7.22 (m, 2H), 7.51−7.59 (m, 2H), 7.85−7.86 (d, 1H). Anal. ($C_{14}H_9N_3OS$) C, H, N.

2-Amino-4,6-difuran-2-yl-nicotinonitrile (44, LUF6080). mp: 199 °C. ^1H NMR $\delta(CDCl_3)$: 5.30 (s, 2H), 6.55 (m, 2H), 7.46 (d, 1H), 7.51 (s, 1H), 7.58 (d, 1H). Anal. ($C_{14}H_9N_3O_2$) C, H, N.

Biology

Binding Studies. [^{3}H]DPCPX and [^{125}I]AB-MECA were purchased from Amersham Biosciences (NL). [^{3}H]ZM241385 (4-(2-[7-amino-2-(2-furyl)[1,2,4]triazolo[2,3-α][1,3,5]triazin-5-ylamino]ethyl)phenol) and [^{3}H]MRS1754 (*N*-(4-cyanophenyl)-2-[4-(2,6-dioxo-1,3-dipropyl-2,3,4,5,6,7-hexahydro-1*H*-purin-8-yl)-phenoxy]acetamide) were obtained from Tocris Cookson, Ltd. (UK). CHO cells expressing the human adenosine A_1 receptor were provided by Dr. Andrea Townsend-Nicholson, University College London, UK. Dr. S. Rees (GSK, Stevenage, UK) kindly provided CHO cells expressing the human A_{2B} receptor. HEK293 cells stably expressing the human adenosine A_{2A} and A_3 receptor were kind gifts from Dr. J. Wang (Biogen/IDEC, Cambridge, MA) and Dr. K. N. Klotz (University of Würzburg, Germany), respectively.

All compounds were tested in radioligand binding assays to determine their affinities at human adenosine A_1 ([^{3}H]DPCPX), A_{2A} ([^{3}H]ZM241385), and A_3 ([^{125}I]AB-MECA) receptors as described previously in literature with the exception that nonspecific binding to the A_{2A} receptor was determined in the presence of 10 μM CGS21680 instead of 100 μM CPA. For the adenosine A_{2B} receptor assay membranes containing 11 μg of protein were incubated in a total volume of 100 μL of 50 mM Tris/HCl, 0.1% CHAPS, ADA 0.8 IU/mL (pH 7.4) and [^{3}H[MRS1754 (final concentration, 1.2 nM) for 1 h at 25 °C in a shaking water bath. Nonspecific binding was determined in the presence of 1 μM NECA. The incubation was terminated by filtration over Whatman GF/C filters under reduced pressure with a Brandel harvester (Gaithersburg, MD). Filters were washed three times with ice cold 50 mM Tris/HCl pH 7.4, placed in vials and counted.

cAMP assay. HEK293 cells expressing the human A_{2A} adenosine receptor were grown as a monolayer on 6 cm culture plates. The cells were harvested and centrifuged two times for 5 min/1000 rpm. For cAMP production and determination, 7500 cells/well were used on 384-well plates. The cells were incubated for 45 min at room temperature with either CGS21680 alone or together with compound **44** in different concentrations. The assay medium also contained cilostamide (50 μM), rolipram (50 μM), and adenosine deaminase (0.8 IU/mL). Incubation was stopped with detection mix and antibody solution was added, these two steps according to the instructions of the supplier. The assay was performed with the Lance cAMP 384 kit from Perkin-Elmer based on the competition of the sample's cAMP with a europium-labeled cAMP tracer complex for binding sites on cAMP-specific antibodies labeled with Alexa Fluor dye.

Data Analysis. K_i values were calculated using a nonlinear regression curve fitting program (GraphPad Prism 4.0, GraphPad Software Inc., San Diego, CA). K_i values of radioligands were 1.6, 1.0, 1.3, and 5.0 nM for [^{3}H]DPCPX, [^{3}H]ZM 241385, [^{3}H]MRS1754, and [^{125}I]AB-MECA, respectively.

Supporting Information Available: ^{1}H NMR data of compounds **1−16.** Physical data and elemental analysis of the target compounds **17−45**. This material is available free of charge via the Internet at http://pubs.acs.org.

References

(1) Moreau, J.-L.; Huber, G. Central adenosine A_{2A} receptors: an overview. *Brain Res. Rev.* **1999**, *31*, 65–82.

(2) Xu, K.; Bastia, E.; Schwarzschild, M. Therapeutic potential of adenosine A_{2A} receptor antagonists in Parkinson's disease. *Pharmacol. Ther.* **2005**, *105*, 267–310.

(3) Jacobson, K. A.; Gao, Z.-G. Adenosine receptors as therapeutic targets. *Nat. Rev. Drug Discovery* **2006**, *5*, 247–264.

(4) Hockemeyer, J.; Burbiel, J. C.; Muller, C. E. Multigram-Scale Syntheses, Stability and Photoreactions of A_{2A} Adenosine Receptor Antagonists with 8-Styrylxanthine Structure: Potential Drug for Parkinson's Disease. *J. Org. Chem.* **2004**, *69*, 3308–3318.

(5) Ongini, E.; Dionisotti, S.; Gessi, S.; Irenius, E.; Fredholm, B. B. Comparison of CGS15943, ZM 241385 and SCH 58261 as antagonists at human adenosine receptors. *Naunyn-Schmiedebergs Arch. Pharmacol.* **1999**, *359*, 7–10.

(6) Matasi, J. J.; Caldwell, J. P.; Hao, J.; Neustadt, B.; Arik, L.; Foster, C. J.; Lachow, J. The discovery and synthesis of novel adenosine receptor (A_{2A}) antagonists. *Bioorg. Med. Chem. Lett.* **2005**, *15*, 1333–1336.

(7) Dowling, J. E; Vessels, J. T.; Haque, S.; Chang, H. X; van Vloten, K; Kumaravel, G; Engber, T.; Jin, X.; Phadke, D.; Wang, J.; E., A.; Petter, R. C. Synthesis of [1,2,4]triazolo[1,5-α]pyrazines as adenosine A_{2A} receptor antagonists. *Bioorg. Med. Chem. Lett.* **2005**, *15*, 4809–4813.

(8) Matasi, J. J.; Caldwell, J. P.; Zhang, H.; Fawzi, A.; Cohen-Willams, M.E.; Varty, G.B.; Tulshian, D.B. 2-(2-Furanyl)-7-phenyl[1,2,4]triazolo[1,5-*c*]pyrimidin-5-amine analogs: Highly potent, orally active, adenosine A_{2A} antagonists. Part 1. *Bioorg. Med. Chem. Lett.* **2005**, *15*, 3670–3674.

(9) Matasi, J. J.; Caldwell, J. P.; Zhang, H.; Fawzi, A.; Higgins, G. A.; Cohen-Willams, M. E.; Varty, G. B.; Tulshian, D. B. 2-(2-Furanyl)-7-phenyl[1,2,4]triazolo[1,5-*c*]pyrimidin-5-amine analogs as adenosine A_{2A} antagonists: The successful reduction of hERG activity. Part 2. *Bioorg. Med. Chem. Lett.* **2005**, *15*, 3675–3678.

(10) Yao, G.; S., H.; Sha, L.; Kumaravel, G.; Wang, J.; Engber, T. M.; Whalley, E. T.; Conlon, P. R.; Chang, H.; Keisman, W. F.; Petter, R. C. Synthesis of alkyne derivatives of a novel triazolopyrazine as A_{2A} adenosine receptor antagonists. *Bioorg. Med. Chem. Lett.* **2005**, *15*, 511–515.

(11) Hairruo, P.; Kumaravel, G.; Sha, L.; Wang, J.; van Vlijmen, H.; Bohnert, T.; Huang, C.; Vu, C. B.; Ensinger, C. L.; Chang, H.; Engber, T. M.; Whalley, E. T.; Petter, R. C. Novel Bicyclic Piperazine Derivatives of Triazolotriazine and Triazolopurimidines as Highly Potent and Selective Adenosine A_{2A} Receptor Antagonists. *J. Med. Chem.* **2004**, *47*, 6218–6229.

(12) Collotta, V.; Catarazi, D.; Varano, F.; Filacchioni, G.; Martini, C.; Trincavelli, L.; Lucacchini, A. Synthesis of 4-Amino-6-(hetero)arylalkylamino-1,2,4-triazolo[4,3,-α]quinoxalin-1-one Derivatives as Potent A_{2A} Adenosine Receptor Antagonists. *Bioorg. Med. Chem.* **2003**, *11*, 5509–5518.

(13) Alanine, A.; Anselm, L.; Steward, L.; Thomi, S.; Vifian, W.; Groaning, M. D. Synthesis and SAR evaluation of 1,2,4-triazoles as A_{2A} receptor antagonists. *Bioorg. Med. Chem. Lett.* **2004**, *14*, 817–821.

(14) Baraldi, P. G.; Fruttarolo, F.; Tabirizi, M. A.; Preti, D.; Romagnoli, R.; El-Kashef, H.; Moorman, A.; Varani, K.; Gessi, S.; Merighi, S.; Borea, P. A. Design, Synthesis, and Biological Evaluation of C^9- and C^2-Substituted Pyrazolo[4,3-*e*]-1,2,4-triazolo[1,5-*c*]pyrimidines as New A_{2A} and A_3 Adenosine Receptors Antagonists. *J. Med. Chem.* **2003**, *46*, 1229–1241.

(15) Baraldi, P. G.; Cacciari, B.; Romagnoli, R.; Spalluto, G.; Monopoli, A.; Varani, K.; Borea, P. A. 7-Substituted 5-Amino-2-(2-furyl)pyrazolo[4,3-*e*]-1,2,4-triazolo[1,5-*c*]pyrimidines as A_{2A} Adenosine Receptor Antagonists: A Study on the Importance of Modifications at the Side Chain on the Activity and Solubility. *J. Med. Chem.* **2002**, *45*, 115–126.

(16) Vu, C. B.; Pan, D.; Peng, B.; Sha, L.; Kumaravel, G.; Jin, X.; Phadke, D.; Engber, T.; Huang, C.; Reilly, J.; Tam, S.; Petter, R. C. Studies on adenosine A_{2a} receptor antagonists: comparison of three core heterocycles. *Bioorg. Med. Chem. Lett.* **2004**, *14*, 4831–4834.

(17) Weiss, S. M.; Benwell, K.; Cliffe, I. A.; Gillespie, R. J.; Knight, A. R.; Lerpiniere, J.; Misra, A.; Pratt, R. M.; Revell, D.; Upton, R.; Dourish, C. T. Discovery of nonxantine adenosine A_{2A} receptor antagonists for the treatment of Parkinson's disease. *Neurology* **2003**, *61*, 101–106.

(18) Minetti, P.; Tinti, M. O.; Carminati, P.; Castorina, M.; Di Cesare, M. A.; Di Serio, S.; Gallo, G.; Ghirardi, O.; Giorgi, F.; Giorgi, L.; Piersanti, G.; Bartoccini, F.; Tarzia, G. 2-*n*-Butyl-9-methyl-8-[1,2,3]triazolo-2-yl-9*H*-purine and Analogues as A_{2A} Adenosine Receptor Antagonists. Design, Synthesis, and Pharmacological Characterization. *J. Med. Chem.* **2005**, *48*, 6887–6896.

(19) Yang, M.; Soohoo, D.; Soelaiman, S.; Kalla, R.; Zablocki, J.; Chu, N.; Leung, K.; Yao, L.; Diamond, I.; Belardinelli, L.; Shryock, J. C. Characterization of the potency, selectivity, and pharmacokinetic profile for six adenosine A_{2A} receptor antagonists. *Naunyn-Schmiedebergs Arch. Pharmacol.* **2007**, *375*, 133–144.

(20) Silverman, L. S.; Caldwell, J. P.; Greenlee, W. J.; Kiselgof, E.; Matasi, J. J.; Tulshian, D. B.; Arik, L.; Foster, C.; Bertorelli, R.; Monopoli, A.; Ongini, E. 3*H*-[1,2,4]-Triazolo[5,1-*i*]purin-5-amine derivatives as adenosine A_{2A} antagonists. *Bioorg. Med. Chem. Lett.* **2007**, *17*, 1659–1662.

(21) *Spartan '04*; Wavefunction Inc.: Irvine, CA, 2005.

(22) Wei, J.; Wang, S.; Gao, S.; Dai, X.; Gao, Q. 3D-pharmacophore models for selective A_{2A} and A_{2B} adenosine receptor antagonists. *J. Chem. Inf. Model.* **2007**, *47*, 613–625.

(23) Richardson, C. M.; Gillespie, R. J.; Williamson, D. S.; Jordan, A. M.; Fink, A.; Knight, A. R.; Sellwood, D. M.; Misra, A. Identification of non-furan containing A_{2A} antagonists using database mining and molecular similarity approaches. *Bioorg. Med. Chem. Lett.* **2006**, *16*, 5993–5997.

(24) Murata, T.; Shimada, M.; Sakakibara, S.; Yoshino, T.; Kadono, H.; Masuda, T.; Shimazaki, M.; Shintani, T.; Fuchikami, K.; Sakai, K.; Takeshita, H. I. K.; Niki, T.; Umeda, M.; Bacon, K. B.; Zeigelbauer, K. B.; Lowinger, T. B. Discovery of Novel and Selective Ikk-β Serine-Threonine Protein Kinase Inhibitors Part 1. *Bioorg. Med. Chem.* **2003**, *13*, 913–918.

(25) Kambe, S.; Saito, K. A Simple Method for the Preparation of 2-Amino-4-Aryl-3-Cyanopyridines by the Condensation of Malononitrile with Aromatic Aldehydes and Alkyl Ketones in the Presence of Ammonium Acetate. *Synthesis* **1980**, *6*, 366–368.

(26) Cowart, M.; Lee, C.-H.; Gfesser, G. A.; Bayburt, E. K.; Bhagwat, S. S.; Stewart, A. O.; Yu, H.; Kohlhaas, K. L.; McGaraughty, S.; Wismer, C. T.; Mikusa, J.; Zhu, C.; Alexander, K. M.; Jarvis, M. F.; Kowaluk, E. A. Structure−Activity Studies of 5-Substituted Pyridopyrimidines as Adenosine Kinase Inhibitors. *Bioorg. Med. Chem. Lett.* **2001**, *11*, 83–86.

(27) Topliss, J. G. Utilization of Operational Schemes for Analog Synthesis in Drug Design. *J. Med. Chem.* **1972**, *15*, 1006–1011.

(28) Anderson, D. R.; Stehle, N. W.; Kolodziej, S. A.; Reinhard, E. J. Preparation of aminocyanopyridines as inhibitors of mitogen activated protein kinase-activated protein kinase-2 for treating TNFα mediated diseases. WO 2004/055015 A1, 2004.

(29) Lameijer, E. W.; Kok, J. N.; Bäck, T; IJzerman, A. P. The Molecule Evoluator. An interactive evolutionary algorithm for the design of drug-like molecules. *J. Chem. Inf. Model.* **2006**, *46*, 545–552.

(30) Lameijer, E. W.; Tromp, R. A.; Spanjersberg, R. F.; Brussee, J.; IJzerman, A. P. Designing active template molecules by combining computational de novo design and human chemist's expertise. *J. Med. Chem.* **2007**, *50*, 1925–1932.

(31) Lipinski, C. A.; Lombardo, F.; Dominy, B. W.; Feeney, P. J. Experimental and computational approaches to estimate solubility and permeability in drug discovery and development settings. *Adv. Drug Delivery Rev.* **1997**, *23*, 3–25.

JM701594Y